

High-valent metalloporphyrins in hydrocarbon activation: metal(v)-oxo or metal(v)-hydroxo?

Radu Silaghi-Dumitrescu*

Received (in Montpellier, France) 20th April 2010, Accepted 24th June 2010

DOI: 10.1039/c0nj00297f

Mn(v) porphyrins featuring an oxo ligand *trans* to a hydroxo group offer a unique opportunity to compare the hydrogen atom abstraction ability of a protonated vs. a non-protonated high-valent oxo metal species, providing insight into the issue of oxo ligand protonation in Fe-containing biologically high-valent centers. Such a comparison is performed here by means of density functional calculations (DFT) on the manganese complex alongside with its Fe-containing counterpart (Fe(v)-oxo-hydroxo heme), showing that, regardless of the metal and within the same complex, both the oxo and the hydroxo ligands are very much able to abstract a hydrogen atom from a hydrocarbon (activation energies under 25 kcal mol⁻¹).

High-valent heme Fe species in enzymes, formally Fe(IV) and Fe(V), are known in biology to harbour an oxo ligand to the Fe *trans* to a protein-derived ligand, and are often referred to as Compound I and Compound II.^{1–6} These Compounds exhibit strong oxidizing activity, either by simple outer-sphere electron transfer, oxygen atom transfer to a heteroatom or to a carbon–carbon multiple bond, or by hydrogen atom abstraction, usually as part of an oxygen atom insertion into a carbon–hydrogen bond.^{1–6} It has more recently been shown that at least some of these high-valent species can protonate at the oxo atom, generating an Fe(IV)-hydroxo form. Thus, Green and co-workers have employed X-ray absorption spectroscopy (EXAFS), resonance Raman, electron paramagnetic resonance (EPR) coupled to cryoradiolysis, Mössbauer spectroscopy and density functional calculations (DFT) to show that thiolate-ligated Compound II species, but not imidazole-ligated examples, are always protonated under physiological conditions.^{3,7–9} Crystallographic and spectroscopic evidence from Poulos and co-workers,¹⁰ as well as from Hersleth *et al.*,^{5,11} suggest that histidine-ligated Compound II-type species are also always protonated, at odds, however, with the data from Green and co-workers. We have shown that globin Compound II electron-abstracting reactivity is drastically enhanced by a heme-related protonation event, and that, based on MCD and DFT data, this protonation occurs at the oxygen atom with a pK_a of ~4.5.¹² Although to date there is no experimental data to suggest that Compound I species would also be protonated,⁴ DFT results have shown that such a protonated species would exhibit an activation barrier for hydrogen atom abstraction from a hydrocarbon that is very similar to (if not even lower than) its non-protonated counterpart.¹³ This latter

result, together with later data on hydrocarbon activation by Fe–nitrite adducts,¹⁴ provides insight into the mechanism of hydrogen atom abstraction, indicating that the primary factor dictating reactivity would be the redox potential rather than, for instance, the remarkable radical-like electronic structure at the oxygen atom in oxo (non-protonated) ferryl systems.

Mn(v) porphyrins have been well characterized as featuring an oxo ligand *trans* to a hydroxo ligand, and, while forming a remarkable class of oxidants in their own right, are known to exhibit oxidative reactivity similar to that of Compound I species, including hydrogen atom abstraction ability.^{6,15–19} Such Mn(v)-oxo-hydroxo species offer an unique opportunity to compare the hydrogen atom abstraction ability of a protonated vs. a non-protonated oxo high-valent metal species *within* the same adduct. Indeed, Eisenstein and co-workers have recently employed DFT to show that both the oxo and hydroxo ligands in this adduct feature low activation energies for hydrocarbon activation, with the oxo more reactive by ~10 kcal mol⁻¹ than the hydroxo. Here, the related Fe(v)-oxo-hydroxo system is similarly examined in terms of the reactivity at the two ligands, further extending the concept, initially proposed by us,¹³ that protonation of the oxo ligand in ferryl species does not significantly lower their ability to activate hydrocarbons, and that in some cases it may even enhance this reactivity. The lack of reactivity in *S* = 0 Mn(v)-oxo-hydroxo complexes is rationalized as correlating with, but not caused by, the lack of spin density at the oxygen atoms.

Fig. 1 shows the structure of the Mn(v)-oxo-hydroxo porphyrin employed in the present study; as illustrated, a methane molecule is employed as a model hydrocarbon. It can be seen that, as computed at the DFT level (BP86/6-31G**), hydrogen atom abstraction by the *S* = 0 spin state, at either the oxo or hydroxo ligand, requires similar amounts of energy but does not lead to a local minimum and is thus not a viable reaction pathway. On the other hand, in line with previously-reported results on the same system,^{16–19} both the oxo and hydroxo ligands of the *S* = 1 spin state lead to a local minimum on the hydrogen atom abstraction potential surface, with very small estimated energy barriers: ~21 kcal mol⁻¹ for reaction at the hydroxo ligand and 17 kcal mol⁻¹ for reaction at the oxo ligand. Previous reports show similarly low activation energies for the reaction at the oxo atom of the same system, and also cite that no reaction is computed to occur on the *S* = 0 spin state at the oxo atom.^{16–19} This lack of reactivity was found to correlate well with the lack of spin density on the oxygen atom, and hence with a clear oxo (O²⁻) character of the oxygen ligand in the ground state.^{16–19} The data in Fig. 1 importantly

Department of Chemistry and Chemical Engineering, “Babeş-Bolyai” University, Arany Janos Street 11, Cluj-Napoca RO-400028, Romania. E-mail: rsilaghi@chem.ubbcluj.ro

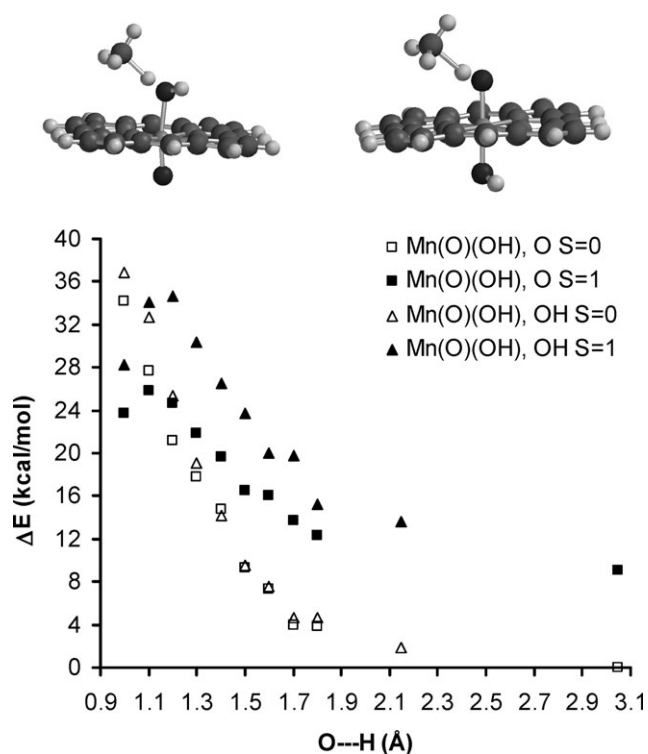


Fig. 1 The structure of the Mn(v)-oxo-hydroxo-porphyrin model used in this study and the DFT energy profile for hydrogen abstraction reactions from a methane molecule. Relative energies are given; the reference point is the $S = 0$ freely optimized model, where the methane sits at ~ 3 Å.

establishes now that the potential energy surface for this reaction is very much accessible, even in the $S = 0$ state, and that the key difference between the $S = 0$ and $S = 1$ spin states is not the energy required to abstract a hydrogen atom from the hydrocarbon, but rather the absence of a local minimum corresponding to product on the $S = 0$ potential energy surface. Such a local minimum would have to feature a methyl radical (as a result of hydrogen atom abstraction from methane), which would, in turn, require an $S = \frac{1}{2}$ state at the metal coupled antiferromagnetically to the methyl radical to achieve the overall $S = 0$ state. Such an electronic structure is most likely unable to lead to a local minimum on the potential surface as the two centers required to be antiferromagnetically coupled would be forced to remain in immediate contact, and would therefore prefer to pair back to a cleanly diamagnetic state. By way of contrast, higher spin states of the Mn(v) adduct would allow the Mn to remain ferromagnetically coupled to the methyl radical, as opposed to antiferromagnetically.

The oxidative reactivity of the Mn(v)-oxo-hydroxo adduct is known to increase upon protonation.¹⁸ This protonation can either occur at the oxo or hydroxo ligand. We have computed the energies of the two di-protonated versions, Mn(v)-oxo-aqua and Mn(v)-hydroxo-hydroxo, finding that the former is slightly favored energetically by ~ 8 kcal mol⁻¹. We interpret this as a consequence of a stronger (hydr)oxo character on the already protonated oxygen ligand, as opposed to the partial oxyl character (hence, less charge) on the non-protonated oxo

ligand. Such an oxyl character is along the lines debated elsewhere for ferryl and related species.^{1,16–25}

Fig. 2 shows similar data to that in Fig. 1, with Fe substituted for Mn, *i.e.* hydrogen atom abstraction from methane by an Fe(v)-oxo-hydroxo heme. Also shown for comparison are the previously-reported¹³ potential energy surfaces for hydrogen atom abstraction from methane by a thiolate-ligated Compound I, in its oxo and hydroxo forms. Unlike in the Mn case, both spin states of the Fe(v)(O)(OH) model lead to a product in the reaction examined. Hydrogen atom abstraction at the oxo ligand requires ~ 18 and 14 kcal mol⁻¹ for the $S = \frac{1}{2}$ and $S = \frac{3}{2}$ spin states, respectively, with the high-spin surface lying 9 kcal mol⁻¹ higher than the low-spin surface. Similar to the Mn case, the barriers for hydrogen atom abstraction by the hydroxo ligand are also small and close to those seen for the oxo: 24 and 11 kcal mol⁻¹, respectively, for the $S = \frac{1}{2}$ and $S = \frac{3}{2}$ spin states. Even though the smallest barrier is seen in the $S = \frac{3}{2}$ model at the hydroxo ligand, this potential energy surface is higher by 10 kcal mol⁻¹ compared to the one involving a reaction at the oxo ligand in the $S = \frac{1}{2}$ state.

A common point of the Mn and Fe potential surfaces is the ~ 9 –10 kcal mol⁻¹ energy difference between the two spin states examined. We have detailed elsewhere²⁶ how such values are close to the experimental error of typical DFT methods, with non-hybrid methods such as BP86 favoring low-spin states. As such, our discussion remains focused on the reactivity of oxo *vs.* hydroxo ligands and not on the exact values of these energy differences between spin states.

In enzymes, the formally Fe(v) species related to our Fig. 2 models are generally accepted to feature a cation radical on the porphyrin ligand coupled ferromagnetically or antiferromagnetically to a formally Fe(IV) center—and this type of structure is well reproduced at the level of theory employed here, including for the models labelled ‘Compound I’ and ‘Compound I-H’ in Fig. 2.^{4,13} Additionally, Green and others have pointed out on a number of occasions that the cation radical may, in principle, delocalize onto the axial ligand *trans* to the oxo—which, in the case of cytochromes P450, is a

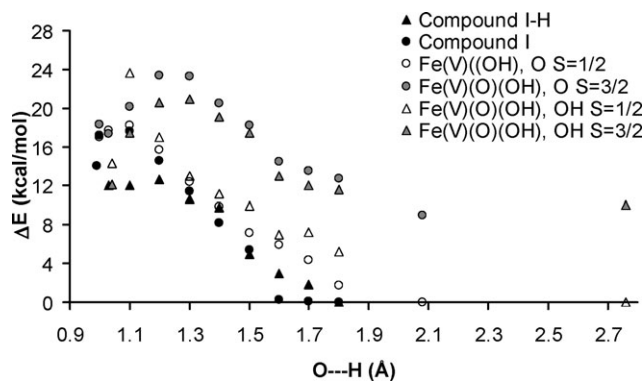


Fig. 2 DFT energy profile for hydrogen abstraction reactions from a methane molecule. The reaction coordinate is the H—O distance between a methane hydrogen atom and either the O or the OH ligand of the Fe. Relative energies are given; the reference point for the Fe(v)(O)(OH) pathways is the $S = \frac{1}{2}$ model freely optimized, where the methane sits at ~ 3 Å away from the oxo oxygen atom.[†]

thiolate.⁴ Fig. 3 now shows that the Fe(v)(O)(OH) models of Fig. 2 are a rare case where a cation radical is not located exclusively on the porphyrin and where the spin density remains localized to a large extent on the O=Fe–OH moiety. An even closer look at the spin densities computed within the two spin states of Fe(v)(O)(OH) (Fig. 3) reveals that the Fe=O moiety does not feature the two unpaired electrons normally seen in other Compound I-like models.^{1,2} Instead, it features 1.25 spin units in the $S = \frac{1}{2}$ state and 2.47 spin units in the $S = \frac{3}{2}$ state. This suggests a significant true Fe(v) character in these complexes, with only a little of the expected radical being seen on the porphyrin and hydroxo ligand (0.25 spin units in the $S = \frac{1}{2}$ state, 0.53 spin units in the $S = \frac{3}{2}$ state, with a notable contribution from the hydroxide ligand in both cases).[‡] For the Mn case, on the other hand, cation radicals on the porphyrin were not expected and a clean Mn(v) character was indeed demonstrated, with less than 0.3 spin units delocalized onto either of the two oxygen ligands, in line with previous data.¹⁹

One notable difference between the Fe and Mn potential energy surfaces shown in Fig. 1 and Fig. 2 is in the degree to which the products are well defined local minima: the Fe systems are at a clear advantage from this point of view. This situation may be rationalized to have a thermodynamic basis in the energy difference between reactants and products—a difference that is smaller in the case of the Fe. Such thermodynamic differences have recently been shown by others to be important in high-valent Fe oxygenating reactions.^{27,28}

The close values seen for hydrogen atom abstraction for the oxo and hydroxo ligands may be interpreted to illustrate the importance of electron affinity as a relevant driving force behind the high reactivity of Fe-bound oxygen ligands towards hydrogen atom abstraction reactions; other factors, such as basicity, or the difference in energy between broken and formed bonds,^{27,28} may have been expected to lead to a somewhat different reactivity between oxo and hydroxo ligands. One can also conclude from the small energy barriers seen for *all* reaction pathways (at the oxo as well as at the hydroxo ligands) and all spin states that the pathways leading to the product will, in practice, be multiple, providing one more example of what has been defined as ‘mechanistic promiscuity’, *i.e.* the ability of a set of reactants to lead to the same product *via* multiple mechanisms¹³—a notion similar to the established multi-state reactivity of Shaik and co-workers,^{22,25} with the observation that in multi-state reactivity, the several reaction channels available may, in principle, lead to different products.

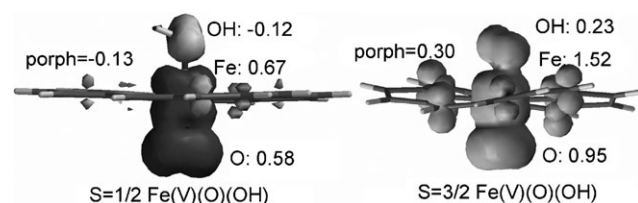


Fig. 3 Spin densities computed for the Fe(v)(O)(OH) models at equilibrium. Spins of opposite signs are shown in different shades of gray.

Methodology

The models consisted of a laterally-unsubstituted porphyrinate bound to Fe or Mn, ligated axially by an oxo ligand *trans* to a hydroxo ligand; the overall charge of the models was always zero to reflect a formally Fe(v)/Mn(v) state. The models were subjected to full geometry optimizations unless otherwise specified. Geometries were optimized for each spin state with the BP86 functional, which uses the gradient-corrected exchange functional proposed by Becke (1988),²⁹ the correlation functional of Perdew (1986)³⁰ and the 6-31G** numerical basis set, as implemented in Spartan.³¹ For the SCF calculations, a fine grid was used, and the convergence criteria were set to 10^{-6} (for the root-mean-square of electron density) and 10^{-8} (energy), respectively. For geometry optimization, convergence criteria were set to 0.001 au (maximum gradient criterion) and 0.0003 (maximum displacement criterion). Charges and spin densities were computed from Mulliken population analyses after DFT geometry optimization. Zero-point, entropy and solvent effects were not computed here. In light of the very small differences between reactants and between mechanisms, these factors are expected to bring about small changes in absolute values but not in trends, and most importantly, not to alter the general conclusion that most barriers examined here are relatively close to each other and, in general, relatively low.

In the relaxed energy scan protocol employed in Fig. 1 and Fig. 2, the reaction coordinate was the H \cdots O distance between a methane hydrogen atom and either the O or the OH ligand of the Mn/Fe. The systems were optimized with the sole constraint on the oxygen–hydrogen distance at values indicated in the Figures. This protocol is expected to yield a reasonable estimate of the barrier heights; a proper transition search would give even more accurate values. The products of the processes illustrated in Fig. 1 and Fig. 2 feature a methyl radical in close contact with a formally Fe(IV)/Mn(IV) center. Not investigated here was the subsequent step of the reaction, in which the methyl radical forms a covalent bond to the metal-bound hydroxide/water. This process is expected to feature a very small reaction barrier due to the free radical nature of one of the reactants, as was also shown previously at the same level of theory for thiolate-ligated Compound I models, both in protonated and non-protonated versions.¹³ Future studies aimed at identifying the exact nature of the final products may have to take into account of the fact that substrates more complicated than methane will offer the possibility of alternative reaction pathways for the carbon-centered radicals generated in Fig. 1 and Fig. 2 other than direct ‘rebound’ on the Fe-coordinated oxygen.

Acknowledgements

Funding from a joint Russian Foundation for Basic Research/Romanian Academy project, as well as from the Romanian government (Ideas project 565/2007), is gratefully acknowledged.

Notes and references

[‡] Values different by 5–10 kcal mol^{−1} were computed for non-protonated Fe(v) models related to those employed here, using non-hybrid functionals with frozen-core basis sets (ref. 28). These differences are

mostly due to the different performances of the two functionals—both directly and indirectly due to the somewhat different electronic structures predicted for the ground states.

‡ In similar models, others have shown (ref. 28) employing a different computational procedure (hybrid B3LYP vs. non-hybrid BP86 used here, with frozen-core vs. non-frozen core basis sets) somewhat different spin densities, with ~ 0.6 – 0.7 spin units on the porphyrin and ~ 0.3 – 0.4 spin units on the hydroxide, thus distinctly closer to a traditional Fe(IV) + cation radical description, and with a stronger contribution from the porphyrin compared to the hydroxide in delocalizing the spin. Such differences between functionals, leading to structures closer to one or another of the two possible electromers, have been noted before in biological metal complexes (e.g., ref. 4 and ref. 26) and certainly require further input from experiment.

- 1 S. Shaik, D. Kumar, S. P. de Visser, A. Altun and W. Thiel, *Chem. Rev.*, 2005, **105**, 2279.
- 2 B. Meunier, S. P. de Visser and S. Shaik, *Chem. Rev.*, 2004, **104**, 3947.
- 3 R. K. Behan and M. T. Green, *J. Inorg. Biochem.*, 2006, **100**, 448.
- 4 R. Silaghi-Dumitrescu, *JBIC, J. Biol. Inorg. Chem.*, 2004, **9**, 471.
- 5 H. P. Hersleth, U. Ryde, P. Rydberg, C. H. Gorbitz and K. K. Andersson, *J. Inorg. Biochem.*, 2006, **100**, 460.
- 6 J. T. Groves, *J. Inorg. Biochem.*, 2006, **100**, 434.
- 7 M. T. Green, J. H. Dawson and H. B. Gray, *Science*, 2004, **304**, 1653.
- 8 M. T. Green, *J. Am. Chem. Soc.*, 2006, **128**, 1902.
- 9 K. L. Stone, R. K. Behan and M. T. Green, *Proc. Natl. Acad. Sci. U. S. A.*, 2006, **103**, 12307.
- 10 C. A. Bonagura, B. Bhaskar, H. Shimizu, M. Sundaramoorthy, D. E. McRee, D. B. Goodin and T. L. Poulos, *Biochemistry*, 2003, **42**, 5600.
- 11 H. P. Hersleth, B. Dalhus, C. H. Gorbitz and K. K. Andersson, *JBIC, J. Biol. Inorg. Chem.*, 2002, **7**, 299.
- 12 R. Silaghi-Dumitrescu, B. J. Reeder, P. Nicholls, C. E. Cooper and M. T. Wilson, *Biochem. J.*, 2007, **403**, 391.
- 13 R. Silaghi-Dumitrescu and C. E. Cooper, *Dalton Trans.*, 2005, 3477.
- 14 R. Silaghi-Dumitrescu and S. V. Makarov, *Eur. J. Inorg. Chem.*, 2010, **7**, 1129.
- 15 F. De Angelis, N. Jin, R. Car and J. T. Groves, *Inorg. Chem.*, 2006, **45**, 4268.
- 16 D. Balcells, C. Raynaud, R. H. Crabtree and O. Eisenstein, *Chem. Commun.*, 2008, 744.
- 17 D. Balcells, P. Moles, J. D. Blakemore, C. Raynaud, G. W. Brudvig, R. H. Crabtree and O. Eisenstein, *Dalton Trans.*, 2009, 5989.
- 18 D. Balcells, C. Raynaud, R. H. Crabtree and O. Eisenstein, *Chem. Commun.*, 2009, 1772.
- 19 D. Balcells, C. Raynaud, R. H. Crabtree and O. Eisenstein, *Inorg. Chem.*, 2008, **47**, 10090.
- 20 R. Silaghi-Dumitrescu, *Proc. Rom. Acad. Ser. B*, 2006, **2–3**, 95.
- 21 R. Silaghi-Dumitrescu, *Studia Univ. Babes-Bolyai, Chimia*, 2005, **50**, 17.
- 22 S. Shaik, S. P. de Visser, F. Ogliaro, H. Schwarz and I. Schröder, *Curr. Opin. Chem. Biol.*, 2002, **6**, 556.
- 23 S. Shaik, S. Cohen, S. P. de Visser, P. K. Sharma, D. Kumar, S. Kozuch, F. Ogliaro and D. Danovich, *Eur. J. Inorg. Chem.*, 2004, 207.
- 24 S. Shaik, S. P. de Visser and D. Kumar, *J. Am. Chem. Soc.*, 2004, **126**, 11746.
- 25 S. Shaik, S. P. de Visser and D. Kumar, *JBIC, J. Biol. Inorg. Chem.*, 2004, **9**, 661.
- 26 R. Silaghi-Dumitrescu and I. Silaghi-Dumitrescu, *Chemtracts: Inorg. Chem.*, 2005, **18**, 595.
- 27 S. Shaik, D. Kumar and S. P. de Visser, *J. Am. Chem. Soc.*, 2008, **130**, 10128.
- 28 S. P. de Visser, *J. Am. Chem. Soc.*, 2010, **132**, 1087.
- 29 A. D. Becke, *Phys. Rev. A: At., Mol., Opt. Phys.*, 1988, **38**, 3098.
- 30 J. P. Perdew, *Phys. Rev. B: Condens. Matter*, 1986, **33**, 8822.
- 31 *Spartan 5.0*, Wavefunction, Inc., 18401 Von Karman Avenue Suite 370, Irvine, CA 92612 USA.